Published in final edited form as:
Br J Ophthalmol. 2010 December ; 94(12): 1618–1623. doi:10.1136/bjo.2009.166843.

Dynamic soft drusen remodelling in age-related macular degeneration

R Theodore Smith[1], **Mahsa A Sohrab**[1], **Nicole Pumariega**[1,2], **Yue Chen**[1], **Jian Chen**[2,3], **Noah Lee**[2], and **Andrew Laine**[2]

[1]Department of Ophthalmology, Harkness Eye Institute, Columbia University, New York, USA

[2]Department of Biomedical Engineering, Fu Foundation SEAS, Columbia University, New York, USA

[3]Institute of Automation, Chinese Academy of Science, Beijing, China

Abstract

Aims—To demonstrate and quantify the dynamic remodelling process of soft drusen resorption and new drusen formation in age-related macular degeneration (AMD) with novel interactive methods.

Methods—Twenty patients with large soft drusen bilaterally and without advanced AMD were imaged at baseline and again at a mean interval of 2 years (40 eyes, 80 images). Each of the 40 serial pairs of images was precisely registered by an automated technique. The drusen were segmented by a user-interactive method based on a background levelling algorithm and classified into three groups: new drusen (only in the final image), resorbed drusen (present initially but not in the final image) and stable drusen (present in both images). We measured each of these classes as well as the absolute change in drusen |D1 – D0| and the dynamic drusen activity (creation and resorption) $D_{new}+D_{resorbed}$.

Results—Mean dynamic activity for the right eye (OD) was 7.33±65.50%, significantly greater than mean absolute change (2.71±2.89%, p=0.0002, t test), with similar results for the left eye (OS). However, dynamic activity OD compared with OS (mean 7.33±5.50 vs 7.91±4.16%, NS) and absolute net change OD versus OS (2.71±2.89 vs 3.46±3.97%, NS) tended to be symmetrical between fellow eyes.

Conclusions—Dynamic remodelling processes of drusen resorption and new drusen formation are distinct disease activities that can occur simultaneously and are not captured by change in total drusen load. Dynamic changes occur at rates more than twice that of net changes, and may be a useful marker of disease activity.

Correspondence to Dr R Theodore Smith, Columbia University Harkness Eye Institute, 160 Ft. Washington Avenue, Room 509C, New York, NY 10032, USA; rts1@columbia.edu.

▶ Supplementary figures are published online only. To view these files please visit the journal online (http://bjo.bmj.com).

Competing interests None.

Ethics approval This study was conducted with the approval of the Institutional Review Board at Columbia University.

Provenance and peer review Not commissioned; externally peer reviewed.

INTRODUCTION

Development of soft drusen is a hallmark of AMD.[1–5] It has also been observed that drusen can resorb spontaneously[6] or in response to laser photocoagulation.[7–9] Despite progress, the biological basis of these processes is not yet understood. It is also not known how the processes of drusen creation and absorption are related temporally or spatially, or indeed to what extent they may be mutually exclusive or can occur simultaneously. Information on these points could in turn shed light on the underlying biology. The reason for this gap is not the lack of photographic raw data, which exists in massive cohort studies such as the Age-Related Eye Disease Study (AREDS) or the Complications of Age-Related Macular Degeneration Prevention Trial (CAPT),[10 11] but rather, the lack of efficient tools for image analysis to assist the human investigator in what would otherwise be an impossibly arduous task. Certainly, the current standard gradings of fundus photographs in AMD,[12] involving manual estimation of drusen loads and locations, have been adequate in many studies[5 6 10 11] to discover important relationships between drusen area and AMD progression. However, precisely sorting drusen into newly formed, resorbed and stable categories is clearly not feasible with side-by-side photographic comparisons.

Herein we propose to dissect the natural history of soft drusen quantitatively into dynamic categories of drusen creation and resorption with a novel digital approach. This approach builds our previously reported system[12–15] into a user-interactive drusen segmentation method and then combines it with a very general automatic retinal image registration technique. This represents three specific advances. First, we take advantage of the human visual system and expert knowledge at the outset to label regions of interest in drusen images for input to the previous automated algorithm. Second, the system now runs independently on a graphical user interface, without the need for additional commercial software. Third, within this interface, we have completely automated registration of serial images for plotting the changing morphology of AMD lesions precisely.

In this paper, we apply all of these techniques to demonstrate and quantify the dynamic remodelling of soft drusen in the natural history of AMD.

METHODS

Subjects

Twenty patients enrolled in the Columbia Macular Genetics Study (CMGS) with bilateral large, soft drusen and without advanced AMD were imaged at baseline and again at a mean interval of 2 years (40 eyes, 80 images). The CMGS is a study of the genetic variations in macular degeneration approved by the Institutional Review Board of New York Presbyterian Hospital (NYPH). All patients were Caucasian and aged >60 years of age.

Image analysis

All image analysis was performed on a desktop PC with an interface linked to Photoshop CS2 (version 9.0.2; Adobe Systems Inc., San Jose, California, USA) and Matlab R2007 (The Mathworks Inc.; Natick, Massachussetts USA). The region studied was the central 6000 μm diameter circle (the central and middle and outer subfields of diameters 1, 3 and 6mmdefined by the Wisconsin grading template[2 3]). All area measurements are stated as percentages of these circles. This macula–disc distance (3000 μm) is established as the constant of reference in clinical macular grading systems.[1 2] Although this distance varies anatomically,[16] it does not affect area measurements as percentages.

Each of the 40 serial pairs of images was precisely registered by an automated image registration technique (figure 1),[17 18] and the drusen in each image pair were segmented by a

user-interactive method based on a background levelling algorithm described previously (figure 2).[11–14 19] Details of registration and segmentation are in the next two sections. These steps are implemented in a graphical user interface (figure 3). Comparing the initial (D0) and final (D1) drusen segmentations in registration then provided an immediate classification of drusen (or parts of drusen) into three classes: new drusen (present only in D1), resorbed drusen (present in D0 but not in D1) and stable drusen (present in both images) We measured each of these three classes, as well as the net change in drusen D1 – D0, absolute change in drusen |D1 – D0|, and the dynamic drusen activity (creation and resorption) $D_{new}+D_{resorbed}$ (figure 4).

Image registration

In order to accurately compare the 40 serial pairs of drusen fundus images, we used a novel, completely automated registration algorithm based on a highly distinctive local feature descriptor (Intensity Invariant Feature Descriptor (IIFD)).[17 18] Prior algorithms for image registration have been unable to register multimodal image pairs in which the vasculature is severely affected by noise and artefacts.[20] The IIFD is invariant to image rotation and image intensity while also being partially invariant to image scaling and affine transformation, making it effective for multimodal retinal image registration. The ability of the IIFD to match correlated image areas with structural outlines of similar behaviour while rejecting a match between differing areas with divergent structural outlines is the basis for its ability to support the multimodal image registration of retinal images with varying quality, including those of poor quality. If the characteristics of the two images are too diverse, then the user can direct the algorithm to consider only the vasculature. This algorithm is thus able to register an autofluorescence (AF), infrared (IR), colour photographic or fluorescein angiographic (FA) image of a given eye to another such image of any of these types (AF to IR, colour to FA, etc). For details on method and validation, see Pumariega *et al*.[17]

We tested accuracy by superimposing the initial and final drusen images in Adobe Photoshop as a layered image (Adobe Systems Inc.) and flickering one of them on and off the second one. Testing was performed by members of the Department of Biomedical Engineering at Columbia University (RTS, JC, NL, AL), all of whom are specialists in image analysis and were involved in development and review of the software. All of the registrations were termed excellent (major corresponding vessels remained stationary on flicker testing). Registered image pairs were then cropped to the 6000 μm region using an auto-crop tool in preparation for drusen segmentation.[21]

User interactive drusen quantification

Both photographs and AF scans have been extensively analysed by our methods. Our technique employs a mathematical model based on the geometry of fundus reflectance to correct macular background and illumination variability. The first step was to demonstrate that the mathematical model, consisting of quadratic polynomials in several zones with cubic spline interpolation in blending regions between the zones, could approximate the global macular image background of a normal photograph or autofluorescence image with sufficient accuracy to allow its reconstruction and levelling.[13–15 22] The next step was to show that the model, operating on user-defined subsets of background data in abnormal images, was still capable of levelling the background for reliable segmentation of drusen or AF abnormalities accurately.[12 13 15 19 22] For drusen, this method has inter-observer reproducibility and correlates well with retinal experts' drawings.[12] However, highly reflectant structures such as the nerve fibre layer bundles at the arcades, peripapillary atrophy and retinal pigment epithelium (RPE) hypopigmentation, exudates and scars are more likely be mistaken for drusen by the automated method than by an expert grader, requiring postprocessing steps.[12] For this reason we have developed the user-interactive

method, in which the user initially labels regions of interest in drusen images for input to the model that exclude unwanted reflectant structures. The algorithm then computes the background model and final drusen segmentation of the macula with the additional information that no drusen are present outside the region of interest. In practice, for the model this simply means that any unwanted reflectant structures are treated as background and the calculation proceeds as usual, producing a more accurate levelled image. For the drusen segmentation, unwanted reflectant structures have been excluded a priori (figures 2 and 3).

RESULTS

Dynamic drusen activity could be substantial even when the absolute net change in drusen was small. This is illustrated in patient 2, OS (figure 5), and there are many other examples in table 1 and table 2, in which drusen creation and resorption are substantial. Mean dynamic activity for the right eye (OD) was 7.33±5.50%, significantly greater than mean absolute change (2.71±2.89%, p=0.0002, t test), with similarly significant results for the left eye (OS). However, dynamic activity OD compared with OS (mean 7.33±5.50 vs 7.91±4.16%, NS) and absolute net change OD and OS (2.71±2.89 vs 3.46±3.97%, NS) tended to be symmetrical between fellow eyes.

DISCUSSION

Herein the natural history of soft drusen has been dissected quantitatively into dynamic processes of drusen creation and resorption. These processes are distinct disease activities that appear to occur simultaneously in many of the cases examined and are not measured by change in total drusen load. Total dynamic changes (creation plus resorption) over a 2-year interval occurred at rates more than twice that of net changes, and may be a useful marker of AMD disease activity. This result was achieved with a novel digital analysis approach that combined a user interactive method of drusen measurement and an automatic image registration technique. In spite of data presented here, one might still argue that drusen creation and resorption were not happening simultaneously. For this argument, one must postulate that the episodes of drusen creation and resorption for each of the many eyes with substantial changes of both types were separated within the 2-year period of observation. For such slow processes, this seems unlikely.

The new digital approach confers several advantages. The user interactive method offers efficiency in the tedious task of drusen segmentation (requiring about 2 min per image after training), while subsequent image registration allows for the precise monitoring of serial drusen changes. Thus, a single template placed on a registered stack of images ensures that exactly the same regions are being compared in each image. Once this is done, the assessment of the dynamics of drusen resorption and new drusen formation is completely automatic. By comparison, the task of sorting out drusen into newly formed, resorbed and stable categories would be arduous using any side-by-side photographic comparisons. In addition, the presence of any other changing lesion morphologies such as geographical atrophy (GA) could also be superimposed, described and measured. As an example, the CAPT study of laser treatment of bilateral large soft drusen enrolled patients on the basis of drusen load and compared changes in drusen load before and after treatment, concluding that drusen load can be altered by indirect, subthreshold laser treatment.[11] The authors of the study used side-by-side photographic comparisons to determine changes in drusen load,[11] aprocess that could be abetted in future and ongoing clinical trials for drusen and/or dry AMD through the use of automated image analysis techniques such as those presented in our paper. The process of image registration, applied here in the analysis of colour fundus photographs, has proved equally useful in the analysis of other imaging modalities.[19 23]

These and all such methods have several limitations. A source of error in serial comparisons is that the photographic acquisition process introduces distortions, which vary between images and tend to increase peripherally. Image registration provides a remedy for the error resulting from variance between images by forcing subsequent photographs to align to the initial photograph. Hence, measured changes in later photographs relative to the initial are more precise.

A limitation of any method for drusen measurement is the fact that there is no absolutely correct choice for delineating indistinct soft drusen. Even the gold standard, two measurements of the same macula from retinal experts' drawings, can vary by a few per cent.[12] Hence, the expected accuracy of any digital method could be no better. Lesion quantification in human grading of fundus photographs is still more limited. The International Classification asks the grader to mentally aggregate all the drusen in the field in order to form an estimate of the percentage of a macular region occupied by drusen in categories of 0–10%, 10–25%, and so on.[1] In AREDS report number 6,[24] the inter-observer agreement on drusen area was reasonable for these larger categories, but more precise grading requires digital methods.

The significance of the dynamics shown here, for example, simultaneous formation and resorption of drusen in spatially mined. However, it appears certain that the balance between the driving forces for drusen formation and resorption is not spatially uniform throughout the macula in many cases. The analytical tools used here provide a clear picture of the balance of these forces both spatially and temporally. Given that soft drusen formation is such a key indicator of the AMD process, these efficient and accurate tools for monitoring drusen should assist our future exploration of this disease.

Acknowledgments

Supported by grants from The New York Community Trust (New York, USA), National Eye Institute Grant R01 EY015520 (Bethesda, Maryland, USA) and the National Institutes of Health, and unrestricted funds from Research to Prevent Blindness (New York, USA). The funding organisations had no role in the design or conduct of this research.

REFERENCES

1. Bird AC, Bressler NM, Bressler SB, et al. An international classification and grading system for age-related maculopathy and age-related macular degeneration. The International ARM Epidemiological Study Group. Surv Ophthalmol 1995;39:367–74. [PubMed: 7604360]
2. Klein R, Davis MD, Magli YL, et al. The Wisconsin age-related maculopathy grading system. Ophthalmology 1991;98:1128–34. [PubMed: 1843453]
3. Bressler NM, Bressler SB, Seddon JM, et al. Drusen characteristics in patients with exudative versus non-exudative age-related macular degeneration. Retina 1998;8:109–14. [PubMed: 3420311]
4. Smiddy WE, Fine SL. Prognosis of patients with bilateral macular drusen. Ophthalmology 1984;91:271–7. [PubMed: 6201789]
5. Bressler SB, Maguire MG, Bressler NM, et al. Relationship of drusen and abnormalities of the retinal pigment epithelium to the prognosis of neovascular macular degeneration. The Macular Photocoagulation Study Group. Arch Ophthalmol 1990;108:1442–7. [PubMed: 1699513]
6. Bressler NM, Munoz B, Maguire MG, et al. Five-year incidence and disappearance of drusen and retinal pigment epithelial abnormalities. Waterman study. Arch Ophthalmol 1995;113:301–8. [PubMed: 7534060]
7. Abdelsalam A, Del Priore L, Zarbin MA. Drusen in age-related macular degeneration: pathogenesis, natural course, and laser photocoagulation-induced regression. Surv Ophthalmol 1999;44:1–29. [PubMed: 10466585]

8. Little HL, Showman JM, Brown BW. A pilot randomized controlled study on the effect of laser photocoagulation of confluent soft macular drusen [see comments]. Ophthalmology 1997;104:623–31. [PubMed: 9111254]
9. Frennesson IC, Nilsson SE. Effects of argon (green) laser treatment of soft drusen in early age-related maculopathy: a 6 month prospective study. Br J Ophthalmol 1995;79:905–9. [PubMed: 7488578]
10. Age-Related Eye Disease Study Research Group. A randomized, placebo-controlled, clinical trial of high-dose supplementation with vitamins C and E, beta carotene, and zinc for age-related macular degeneration and vision loss: AREDS report no. 8. Arch Ophthalmol 2001;119:1417–36. [PubMed: 11594942]
11. Complications of Age-Related Macular Degeneration Prevention Trial Research Group. Laser treatment in patients with bilateral large drusen: the complications of ARMD Prevention Trial. Ophthalmology 2006;113:1974–86. [PubMed: 17074563]
12. Smith RT, Chan JK, Nagasaki T, et al. Automated detection of macular drusen using geometric background leveling and threshold selection. Arch Ophthalmol 2005;123:200–6. [PubMed: 15710816]
13. Smith RT, Nagasaki T, Sparrow JR, et al. A method of drusen measurement based on the geometry of fundus reflectance. Biomed Eng Online 2003;2:10. [PubMed: 12740042]
14. Smith RT, Nagasaki T, Sparrow JR, et al. Photographic patterns in macular images: representation by a mathematical model. J Biomed Opt 2004;9:162–72. [PubMed: 14715069]
15. Smith RT, Chan JK, Nagasaki T, et al. A method of drusen measurement based on reconstruction of fundus background reflectance. Br J Ophthalmol 2005;89:87–91. [PubMed: 15615753]
16. Smith RT, Koniarek JP, Chan J, et al. Autofluorescence characteristics of normal foveas and reconstruction of foveal autofluorescence from limited data subsets. Invest Ophthalmol Vis Sci 2005;46:2940–6. [PubMed: 16043869]
17. Pumariega NM, Chen J, Lee N, et al. Multimodal image registration using the fully automated Harris-invariant feature descriptor. Invest Ophthalmol Vis Sci 2009;50:E-306.
18. Chen J, Smith RT, Tian J, et al. A novel registration method for retinal images based on local features. Conf Proc IEEE Eng Med Biol Soc 2008;2008:2242–5. [PubMed: 19163145]
19. Smith RT, Chan JK, Busuoic M, et al. Autofluorescence characteristics of early, atrophic and high risk fellow eyes in age-related macular degeneration. Invest Ophthalmol Vis Sci 2006;47:5495–504. [PubMed: 17122141]
20. Pluim JPW, Maintz JBA, Viergever MA. Mutual-information-based registration of medical images: a survey. IEEE Trans Med Imaging 2003;22:986–1004. [PubMed: 12906253]
21. Uy K, Smith RT, Busuioc M, et al. Automating drusen analysis with user-friendly graphical interfaces with and without artifact correction. Invest Ophthalmol Vis Sci 2006;47:E-5715.
22. Hwang JC, Chan JW, Chang S, et al. Predictive value of fundus autofluorescence for development of geographic atrophy in age-related macular degeneration. Invest Ophthalmol Vis Sci 2006;47:2655–61. [PubMed: 16723483]
23. Smith RT, Gomes NL, Barile G, et al. Lipofuscin and autofluorescence metrics in progressive Stargardt disease. Invest Ophthalmol Vis Sci 2009;50:3907–14. [PubMed: 19387078]
24. Group A-REDSR. The age-related eye disease study system for classifying age-related macular degeneration from stereoscopic color fundus photographs: the age-related eye disease study report number 6. Am J Ophthalmol 2001;132:668–81. [PubMed: 11704028]

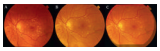

Figure 1.
Registration of serial drusen images. Patient 3 left eye (OS). (A) Initial image. (B) Final image. (C) The initial image has been rotated and rescaled to lie in register with the final. Note the exact vascular correspondence of the overlaid images.

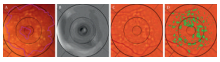

Figure 2.
User interactive segmentation of drusen. (A) Initial image from figure 1 cropped for analysis to the 6000 mm region, with user selected area of drusen. Note that bright area of peripapillary atrophy/hypopigmentation is excluded. (B) Mathematical model of macular background. (C) Levelled image obtained by subtracting mathematical model from (A). Note uniformity of background. (D) Drusen segmentation by uniform threshold.

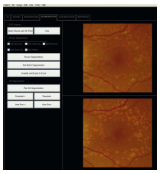

Figure 3.
Screen shot from Graphical User Interface (GUI). Patient 3 left eye (OS). Final image from figure 1 cropped for analysis to the 6000 μm region by the two-click autocrop tool (buttons upper left) in register with the initial image. Above: user selected area of drusen. Below: drusen segmentation.

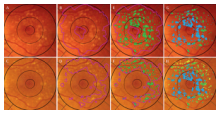

Figure 4.
User interactive drusen segmentation of serial images and dynamic classification. Registered images from figure 1 cropped for analysis to the 6000 μm region. Top row, initial image; bottom row, final image. (A) Initial image, original. (B) Initial image, user selected area of drusen (magenta). Note that bright area of peripapillary atrophy/hypopigmentation is excluded. (C) Final image, original. (D) Final image, user-selected area of drusen. (E) Initial image, drusen segmentation (14.83%, green) obtained by mathematical model applied to user-defined region. (F) Final image, drusen segmentation (7.74%, green). (G) By comparison of initial to the final segmentation, the initial drusen segmentation is subdivided into stable (4.31%, green) and resorbed (10. 51%, blue). (H) Final drusen segmentation, subdivided into stable (4.31%, green) and new (3.43%, yellow), with resorbed (10.51%, blue) overlaid.

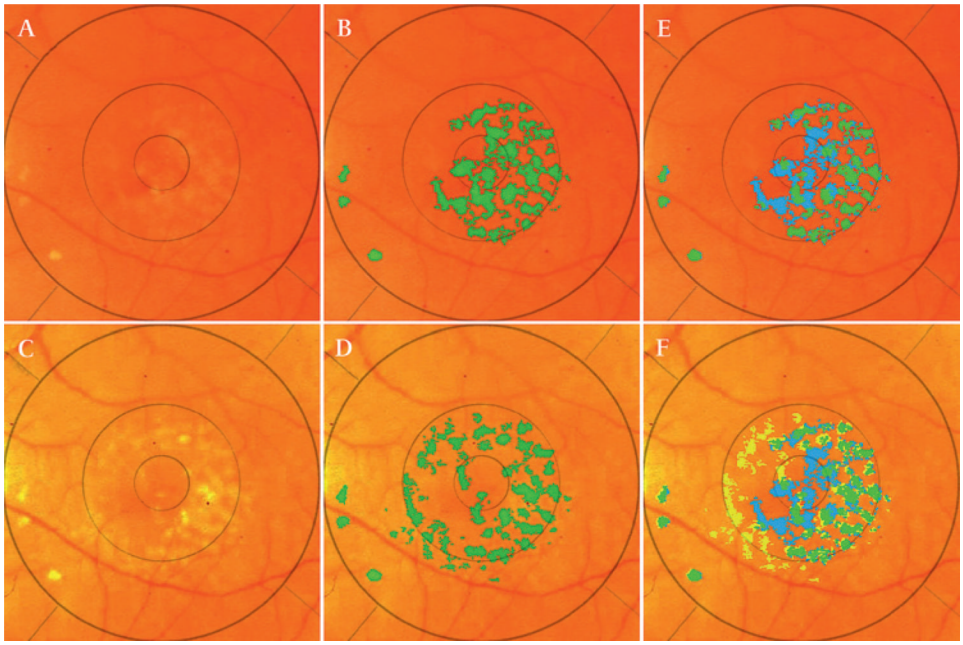

Figure 5.
Drusen remodelling: total mass versus dynamic, simultaneous activity. Patient 2 left eye (OS). Top row, initial image. Bottom row, final image. (A) Initial image, original. (B) Initial image, drusen segmentation (green). (C) Final image, original. (D) Final image, drusen segmentation. (E) By comparison of initial to the final segmentation, the initial drusen segmentation is subdivided into stable (green) and resorbed (blue). (F) Final drusen segmentation, subdivided into stable (green) and new (yellow), with resorbed (blue) overlaid. In this case, while the change in total drusen mass is exactly zero (drusen occupy 7.7% of the 6000 mm circle in both the initial and final images), dynamic drusen activity is significant: mass drusen resorption has taken place centrally (3.7%, blue) and simultaneously new drusen formation has occurred nasally (3.7%, yellow). The dynamic drusen activity is 7.4%.

Table 1

Soft drusen dynamics versus net drusen change in 40 study eyes (right eye)

	Right eye (OD)						
Patient no.	**New**	**Stable**	**Resorbed**	**Initial**	**Final**	**Dynamic**	**Abs net**
1	1.18	6.32	1.15	7.47	7.50	2.34	0.03
2	7.21	0.32	0.04	0.36	7.53	7.25	7.17
3	10.36	21.86	8.20	30.06	32.22	18.56	2.16
4	0.94	3.78	0.60	4.38	4.72	1.54	0.35
5	8.36	8.65	2.37	11.02	17.00	10.73	5.98
6	1.00	1.21	6.00	7.20	2.21	7.00	4.99
7	0.10	0.07	0.17	0.24	0.17	0.27	0.07
8	1.00	1.11	0.19	1.30	2.10	1.19	0.81
9	3.14	5.37	3.12	8.49	8.51	6.26	0.01
10	4.30	14.09	15.24	29.33	18.39	19.54	10.94
11	1.25	2.94	1.84	4.78	4.19	3.09	0.59
12	4.16	18.37	2.68	21.06	22.53	6.84	1.47
13	8.15	22.76	6.45	29.20	30.90	14.59	1.70
14	4.37	23.43	3.85	27.28	27.80	8.22	0.52
15	5.52	3.29	0.70	3.99	8.81	6.21	4.82
16	4.24	5.98	8.70	14.68	10.22	12.94	4.45
17	4.00	9.20	2.78	11.98	13.20	6.78	1.22
18	1.73	0.78	0.17	0.95	2.51	1.90	1.56
19	4.76	4.92	1.24	6.16	9.68	6.00	3.52
20	3.55	8.57	1.78	10.35	12.11	5.33	1.77
Mean	3.97	8.15	3.36	11.15	12.12	7.33	2.71
SD						5.50	2.89

The initial (D0) and final (D1) drusen segmentations in registration were spatially overlaid and digitally compared. These provided the classifications: new drusen (present only in D1), resorbed drusen (present in D0 but not in D1), stable drusen (present in both images). The dynamic changes (D_{new}+$D_{resorbed}$) and the absolute net changes |D1 – D0| are also compared. Details of all categories are presented for both eyes. All numbers are per cent area of the 6000 μm region. Abs, absorption.

Table 2

Soft drusen dynamics versus net drusen change in 40 study eyes (left eye)

	Left eye (OS)						
Patient no.	**New**	**Stable**	**Resorbed**	**Initial**	**Final**	**Dynamic**	**Abs net**
1	1.76	7.42	1.57	8.99	9.17	3.33	0.18
2	3.72	3.98	3.73	7.71	7.70	7.45	0.01
3	3.43	4.31	10.51	14.83	7.74	13.94	7.09
4	0.51	1.84	0.44	2.28	2.35	0.95	0.07
5	6.50	7.96	2.78	10.75	14.47	9.29	3.72
6	3.14	5.37	3.12	8.49	8.51	6.26	0.01
7	1.00	1.11	0.19	1.30	2.10	1.19	0.81
8	10.32	9.32	1.75	11.07	19.64	12.07	8.57
9	2.66	5.61	3.76	9.37	8.27	6.42	1.10
10	0.90	2.74	16.13	18.88	3.64	17.03	15.24
11	2.52	3.64	3.77	7.41	6.16	6.29	1.25
12	2.54	3.70	8.27	11.97	6.24	10.81	5.73
13	5.33	27.76	4.92	32.69	33.09	10.25	0.40
14	3.10	23.04	3.00	26.05	26.14	6.11	0.10
15	9.85	8.12	3.53	11.65	17.98	13.38	6.32
16	6.09	4.32	3.30	7.62	10.41	9.39	2.79
17	5.50	6.09	0.85	6.94	11.59	6.35	4.65
18	4.61	0.36	0.05	0.41	4.97	4.66	4.56
19	7.02	5.60	0.47	6.07	12.62	7.49	6.55
20	2.75	7.55	2.76	10.30	10.29	5.51	0.01
Mean	4.16	6.99	3.75	10.74	11.15	7.91	3.46
SD						4.16	3.97

The initial (D0) and final (D1) drusen segmentations in registration were spatially overlaid and digitally compared. These provided the classifications: new drusen (present only in D1), resorbed drusen (present in D0 but not in D1), stable drusen (present in both images). The dynamic changes (D_{new}+$D_{resorbed}$) and the absolute net changes |D1 – D0| are also compared. Details of all categories are presented for both eyes. All numbers are per cent area of the 6000 μm region. Abs, absorption.